EMS527U - Materials Processing and Manufacturing

Case Study 1: Designing a lightweight and strong Bicycle Frame

Name: Sara Hamandi

Student ID: 230346871

Module Code: EMS527U

School Address:
School of Engineering and Materials Science
Queen Mary University of London
Mile End Road
London E1 4NS

Abstract

This report creates and assesses a high-end, all-metal hardtail mountain bike frame with a frame-mass limit of 5 kg for riders weighing up to 100 kg. The study uses EduPack screening, literature evidence, a weighted choice matrix, analytical calculations, and SolidWorks FEA to analyse five candidate alloys: Ti-3Al-2.5V, Ti-6Al-4V, AISI 4130 steel, 6061-T6 aluminium, and AZ31B magnesium. While steel offers dependable toughness and weldability, and aluminium is still appealing for high-volume hydroformed production, both materials are less appealing for a long-lasting off-road frame where performance is determined by fatigue and corrosion resistance. Although magnesium has a very low density, it is not durable enough for wet, impact-prone applications. With a cautious beam-theory safety factor of 2.31 under a 981 N design load, a Goodman fatigue safety factor of 1.87, and full-frame FEA safety factors of at least 4.0 at 981 N and 2.0 at 1962 N, the suggested butted titanium frame is expected to have a bare mass of 1.19 kg. For a premium hardtail application, the strongest processing-property-performance case is provided by a welded Ti-3Al-2.5V frame made using inert-gas welding and precision tube preparation.

Contents

1 Background and Motivation

Hardtail mountain-bike frames are a useful design case because they have to do several things at once: stay light enough for responsive handling and climbing, remain stiff enough for steering accuracy and power transfer, and survive repeated off-road loading without cracking. Unlike a full-suspension bike, a hardtail passes more of the terrain-induced loading directly through the frame, especially through the head tube, down tube, bottom bracket and rear stays. That makes the frame a good example for linking material choice to manufacturing route and then to mechanical performance. Numerical studies of bicycle structures have shown that mountain-bike style loading is not a simple static weight problem; the frame experiences combined bending, torsion and local stress concentration under realistic riding conditions [1, 2]. Experimental and modelling work on MTB loading also shows why fatigue must be treated as a primary design issue rather than an afterthought [3].

For this coursework, the frame must weigh below 5 kg, support a rider of up to 100 kg, and be designed for a specific rider type. These requirements immediately rule out a simplistic "strongest metal wins" approach. In practice, most candidate metals could satisfy the static load requirement if the tube geometry were made heavy enough. The real challenge is achieving low mass while controlling stiffness, welded-joint integrity, fatigue life and environmental durability. Published failure studies reinforce this point. Aluminium bicycle frames have been shown to crack at highly stressed welded regions where local geometry and service stresses interact [4]. Similar work on steel frames tested to ISO 4210 shows that fatigue resistance depends strongly on the behaviour of welded nodes under repeated loading [5].

This report therefore focuses on a premium hardtail mountain bike for an adult rider who values durability, precise handling and long service life over minimum purchase cost. The aim is not only to choose a metal, but to justify a complete material-design route by comparing candidate alloys, considering their processing methods, and evaluating which option gives the best balance of weight, strength, fatigue performance, corrosion resistance and manufacturability.

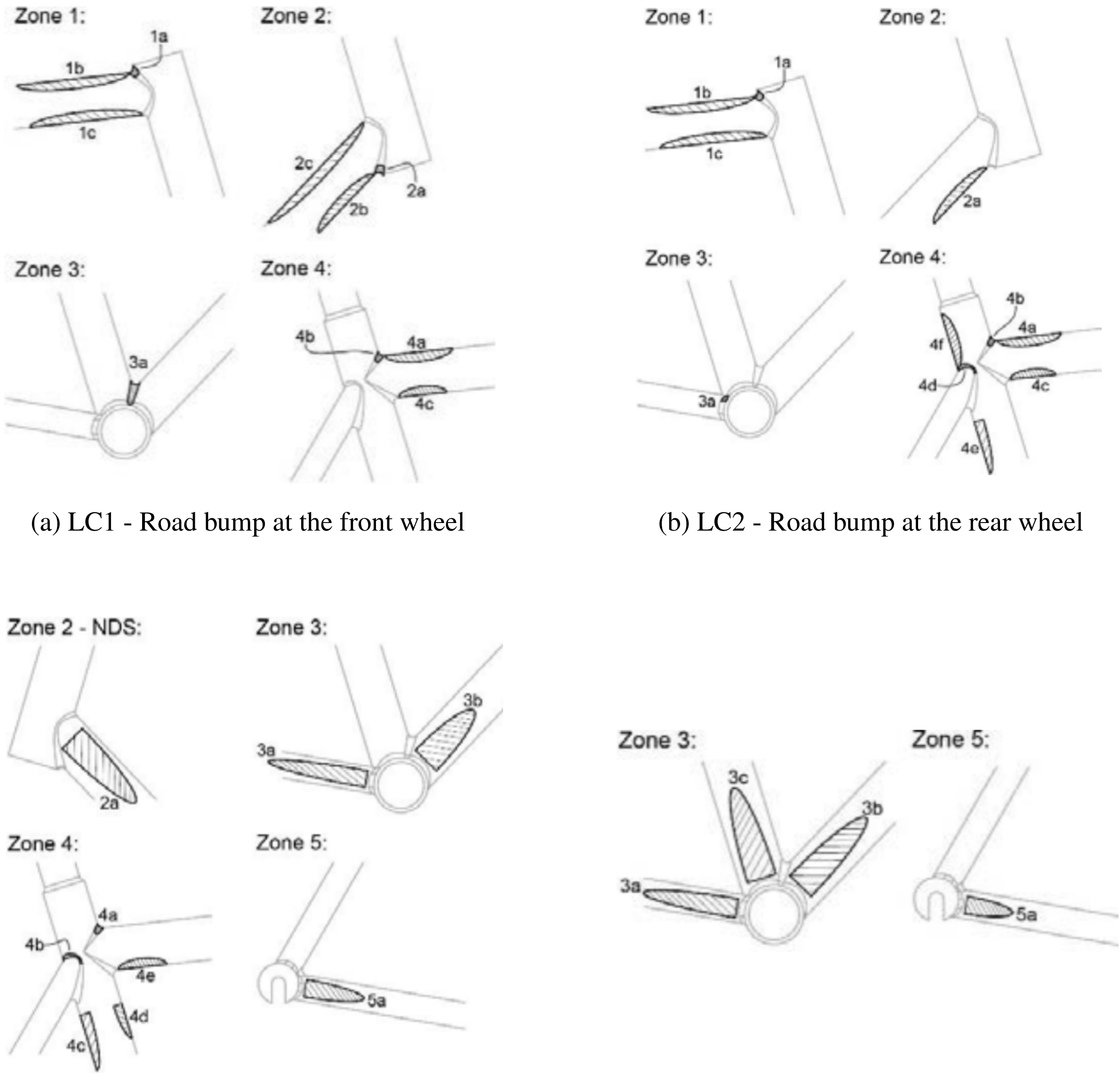

(a) LC1 - Road bump at the front wheel

(b) LC2 - Road bump at the rear wheel

(c) LC3 - Climbing in the saddle

(d) LC4 - Climbing out of the saddle

Figure 1: Loading conditions applied to a bicycle frame in numerical simulation, adapted from [1].

Requirement	Target / Constraint	Design implication
Frame mass	< 5 kg	Favours high specific strength and efficient tube geometry.
Rider mass	Up to 100 kg	Requires adequate static strength and stiffness margin.
Rider type	Hardtail mountain biker	Fatigue, vibration and impact resistance are more important than for road use.
Material class	Metals only	Candidate shortlist limited to titanium, aluminium, steel and magnesium alloys.
Durability	Repeated off-road service	Fatigue strength and weld quality are critical.
Environment	Wet / muddy outdoor use	Corrosion resistance and surface stability are important.
Manufacturing	Real industrial route required	Material must be justifiable using a real company process route.
Design objective	Premium performance	Lifecycle durability can be prioritised over lowest cost.

Table 1: Design requirements and constraints for the proposed hardtail mountain-bike frame.

2 Materials Selection

The final shortlist contains Ti-3Al-2.5V (Grade 9), Ti-6Al-4V (annealed), AISI 4130 normalized steel, 6061-T6 aluminium and AZ31B magnesium alloy. One representative grade was selected from each material family so that the comparison remained controlled and directly relevant to welded bicycle tubing and lightweight structural applications. The decision criteria were specific stiffness, specific strength, fatigue resistance, corrosion resistance, weldability, manufacturability and lifecycle value.

Material	Density (kg/m^3)	E (GPa)	σ_y (MPa)	Fatigue (MPa)	Corrosion rating	Comment
Ti-3Al-2.5V (Grade 9)	4.48e3	93	552	398	High	Main titanium candidate for welded tubing.
Ti-6Al-4V, annealed	4.43e3	114.5	848	354	High	Secondary titanium benchmark; stronger but less ideal for tube fabrication.
AISI 4130, normalised	7.83e3	205	509	323	Moderate	Tough and weldable, but penalised by density.
6061-T6 aluminium	2.71e3	68.3	260	120	Moderate	Lightweight and common in frames; fatigue-sensitive at welded joints.
AZ31B magnesium alloy	1.775e3	45	155	110	Low-Moderate	Very low density, but corrosion and manufacturing concerns remain.

Table 2: Initial shortlist of candidate metallic materials for the bicycle frame with average property values.

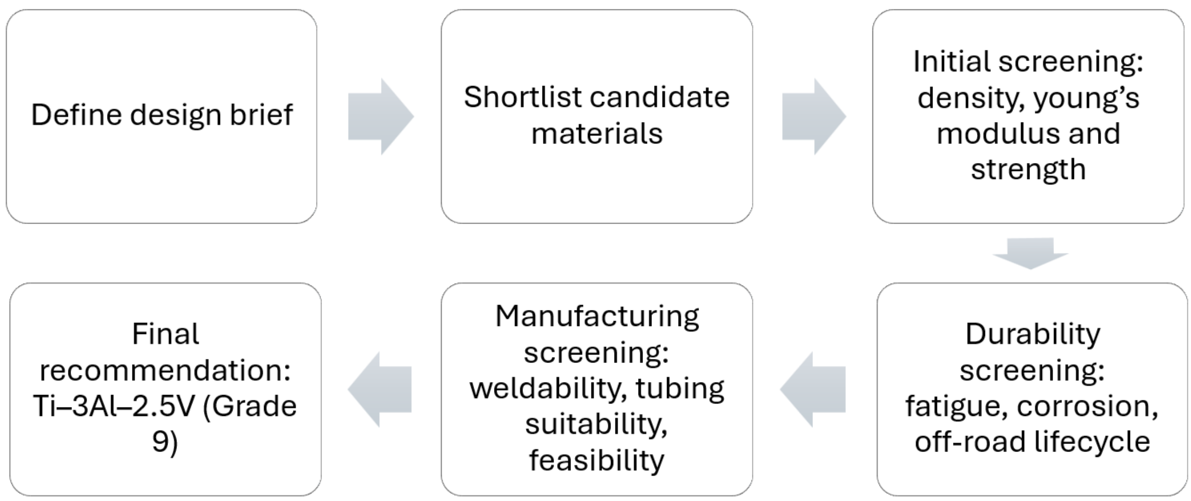

Figure 2: Materials-selection flowchart showing the screening stages used to reduce the metallic shortlist to the final Ti-3Al-2.5V recommendation.

For a premium hardtail bicycle frame, material selection is governed by five linked requirements: mass below 5 kg, sufficient strength for a 100 kg rider, durability under repeated off-road loading, resistance to wet and muddy service, and compatibility with a realistic welded tubular manufacturing route. As a result, the selection cannot be based on absolute strength alone; it must prioritise specific properties, fatigue performance, corrosion resistance and tube manufacturability.

Table 2 and Fig. 2 show the screening logic. AISI 4130 is an appropriate steel benchmark because it offers high stiffness, good weldability and a long history in thin-walled bicycle tubing. Finite-element studies on steel bicycle frames show that tube selection and butting strongly affect frame stiffness and compliance [2]. However, its high density makes it less competitive where premium mass efficiency is required.

6061-T6 aluminium remains an essential comparator because it is widely used in extrusion, welding and hydroforming, and large-diameter thin-walled tubes can deliver high frame stiffness at low mass. Its limitation is welded-joint durability. Soares *et al.* reported multiaxial fatigue damage in welded aluminium joints representative of bicycle frames [6], while Cicero *et al.* documented cracking in an aluminium alloy bike frame [4]. Ambriz *et al.* further showed that weld metal and heat-affected zones in 6061-T6 differ significantly from the base material [7]. Aluminium is therefore attractive for production scale, but less convincing for a long-life high-end hardtail.

AZ31B magnesium alloy offers the lowest density and potentially useful vibration damping, but it is disadvantaged by low modulus and poor corrosion robustness. Liao *et al.* showed that AZ31B corrosion behaviour is strongly affected by microstructure and surface-film stability [8], while later work still depends on coatings and process optimisation to improve service performance [9]. This makes magnesium a weak choice for muddy, impact-prone mountain-bike use.

The final decision therefore lies between the two titanium alloys. Williams and Boyer describe titanium alloys as offering excellent specific strength and corrosion resistance, with Ti-3Al-2.5V specifically identified as a commonly used alloy family for tubing applications [10]. Although Ti-6Al-4V is stronger, it is less formable and more difficult to weld into thin-walled tubes. Ti-3Al-2.5V was therefore selected as the final frame material because it provides the best overall balance of specific strength, fatigue durability, corrosion resistance and welded-tube manufacturability for a premium hardtail bicycle frame.

3 Materials Design Process: Processing and Manufacturing

Moots is a specialist titanium bicycle manufacturer in Colorado whose frames are welded and finished in-house [11]. This makes it a suitable benchmark for analysing a premium Ti-3Al-2.5V tubular manufacturing route.

Route	Manufacturing route	Engineering impact	Suitability
Moots-style titanium	Butted Ti-3Al-2.5V tubes, cutting, mitring, local forming, fixturing, inert-gas welding, finishing and inspection.	Best balance of fatigue resistance, corrosion resistance, low mass and durability, but weld quality depends on shielding control.	Most suitable for a premium hardtail MTB.
Aluminium	6061-T6 tubes made by extrusion or hydroforming, then welded and finished.	Low mass and good production efficiency, but weaker fatigue performance at welded joints.	Suitable, but less durable
Steel	Butted AISI 4130 tubes joined by welding or brazing, then aligned and finished.	Good stiffness, toughness and weldability, but high density increases frame mass.	Credible, but too heavy
Magnesium	AZ31B tubes or formed sections with coating and corrosion protection.	Very low density, but low modulus and poor corrosion resistance reduce reliability.	Least suitable

Table 3: Comparison of the Moots-style Ti-3Al-2.5V frame route with alternative metallic bicycle-frame routes

Table 3 shows that the Moots-style Ti-3Al-2.5V route offers the best balance of fatigue durability, corrosion resistance and low mass for the chosen premium hardtail frame, provided weld shielding and inspection are well controlled.

The suggested frame is a traditional diamond-shaped hardtail composed of butted Ti-3Al-2.5V tubes. Finite-element simulations demonstrate that tube profile and wall thickness significantly affect bicycle-frame stiffness and compliance, which justifies tube butting [2]. While wall thickness is decreased in lower-stress intervals to conserve mass, material is kept close to the head tube, bottom bracket, and seat-cluster regions where bending moments and joint stresses are strongest. While seat stays can be adjusted for comfort without compromising durability, the top and down tubes should be somewhat bigger to regulate front-triangle stiffness.

Precision mitring and local forming come next in an appropriate process chain, which starts with tube selection and cutting. To ensure precise control over joint fit-up, the mitred tubes are put together in a fixture. After joining, alignment checks, surface finishing, and dimensional inspection are carried out utilising a exceptional inert-gas method with thorough shielding. While intervening contamination at high temperatures can weaken the weld region and impair fatigue strength, welding quality plays an important role for titanium. Ucok *et al.* showed that welding can reduce the fatigue strength of titanium tubes relative to base material [12], while Javidrad *et al.* demonstrated that Ti-3Al-2.5V weld quality and microstructure are highly dependent on process control during microplasma arc welding [13]. More thorough analyses of titanium welding further highlight how process variables have a significant impact on microstructure, flaws, and the mechanical performance that results from it [14, 15]. Titanium is an exceptional option only if joint preparation, shielding, and heat input are strictly regulated. This has an apparent significance for frame design.

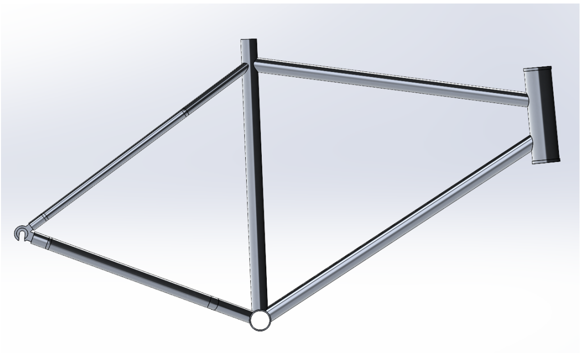

(a) Side view of the frame.

(b) Isometric view of the frame.

Figure 3: CAD engineering views of the proposed hardtail mountain-bike frame.

The CAD model confirms that the proposed hardtail geometry is compatible with a welded tubular Ti-3Al-2.5V manufacturing route, using simple joined sections rather than complex integrated forms.

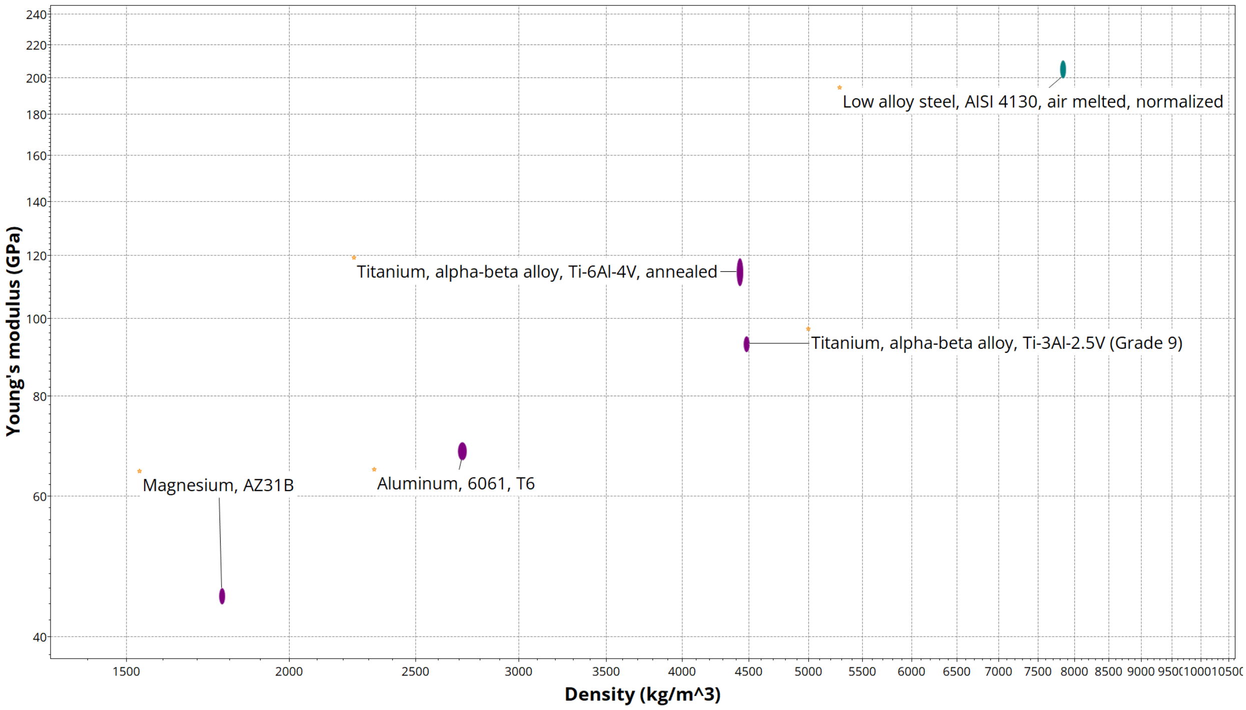

Figure 4: Young's modulus vs density for the shortlisted candidate frame metals

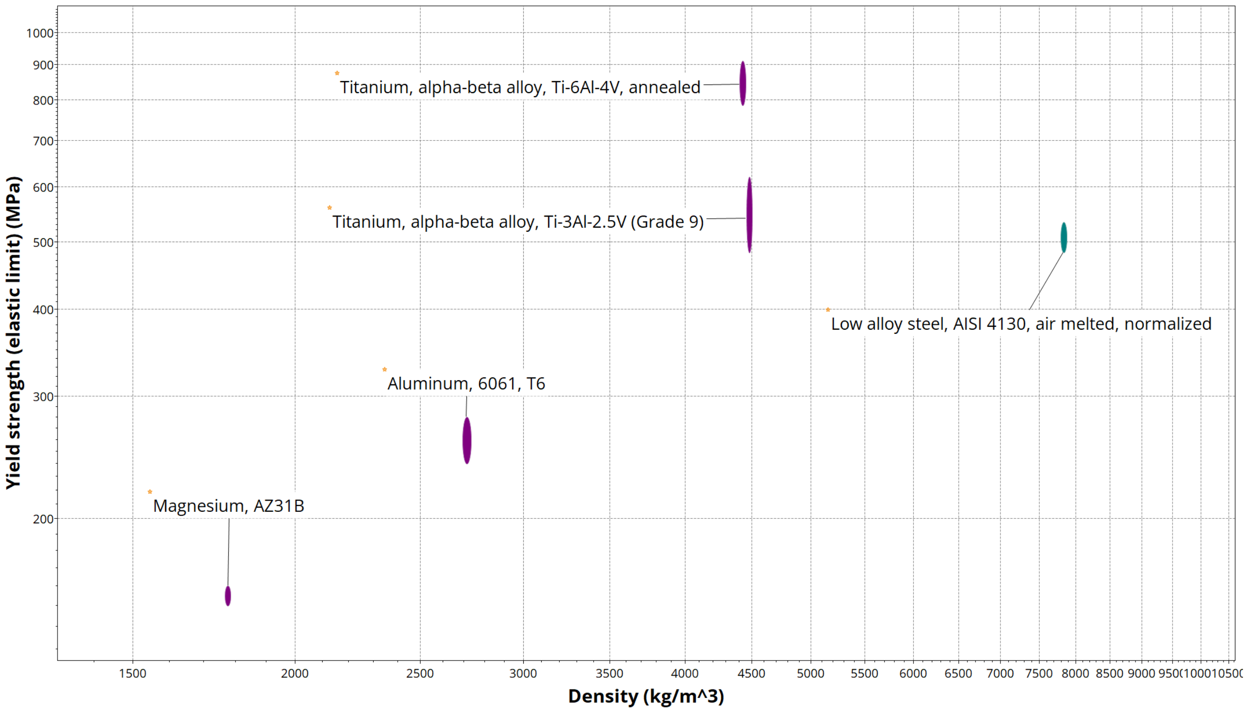

Figure 5: Yield strength vs density for the shortlisted candidate frame metals

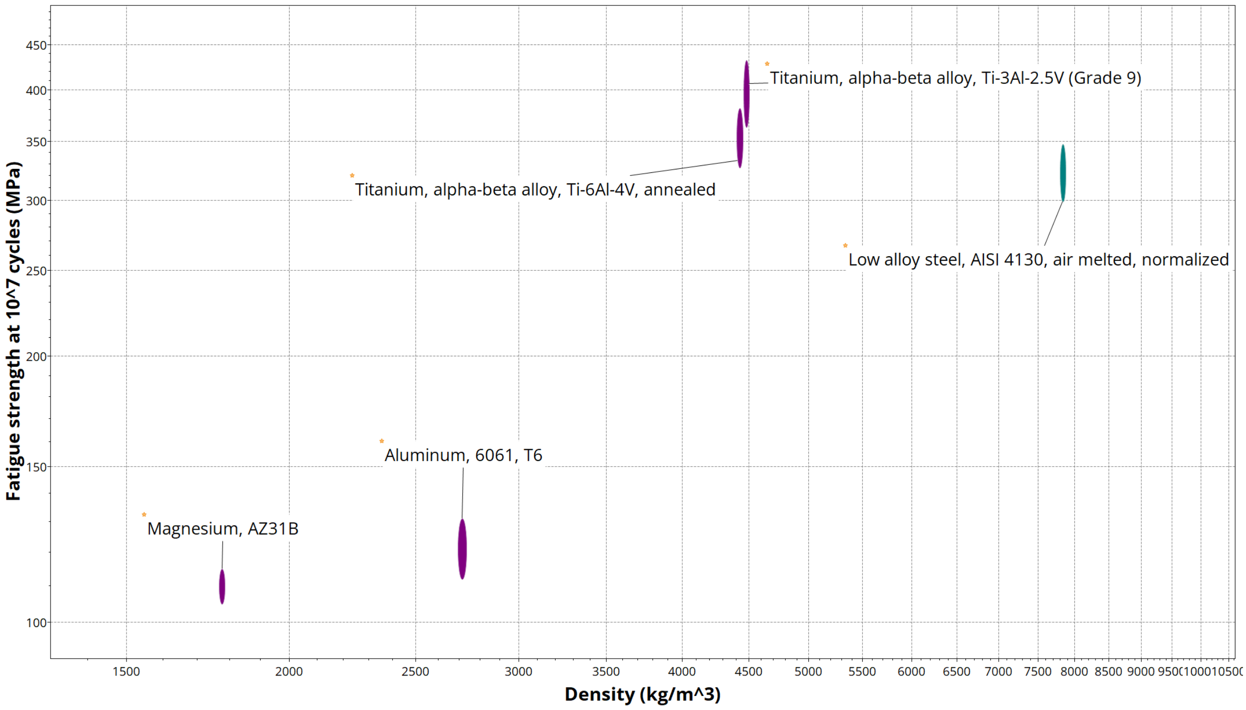

Figure 6: Fatigue strength at 10^7 cycles vs density for the shortlisted candidate frame metals

The EduPack plots (Figures 4-6) visually confirm the material selection detailed in Section 2. Figure 6, in particular, highlights the superior 10^7-cycle fatigue strength of Ti-3Al-2.5V compared to the 6061-T6 aluminium baseline.

4 Results

This section presents the final material-selection outcome and the quantitative performance results for the proposed premium hardtail mountain-bike frame. The results are organised into material screening, weighted ranking, frame-mass verification, analytical stress analysis, fatigue assessment, and full-frame FEA validation.

4.1 Weighted Decision Matrix

Table 4 summarises the weighting logic, and Table 5 presents the full decision matrix. Mass efficiency and fatigue resistance are assigned the highest weights (0.20 each) because the design brief imposes a 5 kg frame limit and the hardtail service case is fatigue-dominated. Cost is assigned the lowest weight (0.05) because the concept is performance-led rather than budget-led.

Criteria	Weight	Justification
Mass efficiency	0.20	A lightweight frame is a primary requirement; total frame mass must remain below 5 kg.
Stiffness efficiency	0.10	Adequate stiffness is required for steering and pedalling efficiency, but is less critical than fatigue durability.
Yield strength	0.10	The frame must safely support a 100 kg rider without permanent deformation.
Fatigue resistance	0.20	Hardtail frames are subjected to repeated cyclic off-road loading, making fatigue one of the most important design criteria.
Corrosion resistance	0.15	The frame will operate in wet and muddy conditions; long-term environmental durability is a key selection factor.
Weldability / fabrication suitability	0.10	The concept is based on welded tubular construction; the material must be compatible with practical manufacturing routes.
Lifecycle durability	0.10	A premium frame concept prioritises long service life and low maintenance beyond initial static performance.
Cost	0.05	Cost remains relevant but receives the lowest weighting because the design is performance-led rather than budget-led.

Table 4: Justification for the weighting factors used in the decision matrix.

Criteria	Weight	Ti-3Al-2.5V	Ti-6Al-4V	AISI 4130	6061-T6	AZ31B
Mass efficiency	0.20	4	4	2	5	5
Stiffness efficiency	0.10	3	4	5	2	1
Yield strength	0.10	4	5	4	2	1
Fatigue resistance	0.20	5	4	4	2	1
Corrosion resistance	0.15	5	5	2	3	1
Weldability / fabrication suitability	0.10	4	2	4	4	1
Lifecycle durability	0.10	5	4	4	2	1
Cost	0.05	1	1	4	5	3
Weighted total	**1.00**	**4.20**	**3.75**	**3.50**	**3.10**	**1.70**

Table 5: Weighted decision matrix used to rank the candidate frame materials. Ti-3Al-2.5V achieves the highest weighted score (4.20) and is selected as the recommended frame alloy.

Ti-3Al-2.5V achieves the highest weighted total (4.20) and is therefore selected as the recommended frame alloy.

4.2 Frame Mass Estimate

The volume of the CAD model was extracted directly from SolidWorks 2025 as $V = 2.653 \times 10^{-4}\ \mathrm{m}^3$. Using the tabulated density of Ti-3Al-2.5V (Grade 9) from Table 2, the predicted bare-frame mass is:

$$m = \rho \cdot V = 4{,}480\ \mathrm{kg\,m^{-3}} \times 2.653 \times 10^{-4}\ \mathrm{m}^3 = \mathbf{1.19}\ \mathrm{kg} \qquad (1)$$

Applying the average raw material cost of £19.95/kg for Ti-3Al-2.5V (Grade 9), the bare titanium tubing for this 1.19 kg frame carries a baseline material cost of approximately £23.74, excluding manufacturing overheads, welding gas, and tooling.

This is 76% below the 5 kg coursework constraint, leaving a remaining mass allowance of

3.81 kg for the bottom bracket shell, dropouts, headset interfaces, cable-routing features and manufacturing allowances.

4.3 Analytical Beam Model

To provide a first-principles structural check, the down tube was modelled as the primary load-carrying member under the seated-climbing load case (LC3, Figure 1). This is a conservative idealisation because the full welded frame shares load across multiple members. The main inputs, assumptions and section properties are summarised in Table 6.

Parameter	**Expression / assumption**	**Value**
Outer diameter	D	28.6 mm
Inner diameter	d	26.8 mm
Tube span	L	500 mm
Wall thickness	t	0.9 mm
Outer fibre distance	$y_{\max} = D/2$	14.3 mm
Cross-sectional area	$A = \frac{\pi}{4}(D^2 - d^2)$	78.3 mm^2
Second moment of area	$I = \frac{\pi}{64}(D^4 - d^4)$	7,518 mm^4
Applied load	100 kg rider, vertical at BB	981 N
Beam idealisation	Simply supported, midspan load	Conservative

Table 6: Analytical beam-model inputs, assumptions and section properties for the down tube.

Using the section properties in Table 6, the maximum bending moment is:

$$M_{\max} = \frac{F \cdot L}{4} = \frac{981 \times 500}{4} = \mathbf{122{,}625}\ \text{N·mm} \tag{2}$$

The corresponding bending stress, axial stress and maximum combined compressive stress are:

$$\sigma_b = \frac{M_{\max} y_{\max}}{I} = \mathbf{233.3}\ \text{MPa} \tag{3}$$

$$\sigma_{\text{axial}} = \frac{F \cos(65^\circ)}{A} = \mathbf{5.3}\ \text{MPa} \tag{4}$$

$$\sigma_{\max} = \sigma_b + \sigma_{\text{axial}} = \mathbf{238.6}\ \text{MPa} \tag{5}$$

Using $\sigma_y = 552$ MPa for Ti-3Al-2.5V (Grade 9), the static safety factor is:

$$n_s = \frac{\sigma_y}{\sigma_{\max}} = \frac{552}{238.6} = \mathbf{2.31} \tag{6}$$

4.3.1 ISO 4210 Dynamic Load Check

ISO 4210 specifies more severe test loads than nominal rider weight [5]. The corresponding beam-model stresses and safety factors are summarised in Table 7.

Test	**Direction**	**Load (N)**	$\sigma_{\max}$ **(MPa)**	n_s
Design load (100 kg rider)	Vertical	981	238.6	2.31
ISO 4210 vertical fatigue	Vertical	1500	356.6	1.55
ISO 4210 combined strength	Vertical	2200	522.7	1.06

Table 7: ISO 4210 test loads for mountain-bike frames and the resulting down-tube stress and safety factor from the analytical beam model.

The reduced safety factors at 1500 N and 2200 N reflect the conservatism of the single-tube idealisation and identify the bottom bracket and head-tube regions as the most critical areas for local reinforcement or butting.

4.4 Modified Goodman Fatigue Analysis

Because repeated service loading is more critical than simple static overload for this application, fatigue was assessed using the Modified Goodman criterion [18, 6, 5]:

$$\frac{\sigma_a}{\sigma_e} + \frac{\sigma_m}{\sigma_{\text{UTS}}} \leq 1 \tag{7}$$

Material constants are listed in Table 8.

Property	**Symbol**	**Value**	**Source**
Endurance limit (10^7 cycles)	σ_e	398 MPa	Table 2
Ultimate tensile strength	σ_{UTS}	620 MPa	[10]
Yield strength	σ_y	552 MPa	Table 2

Table 8: Fatigue material properties for Ti-3Al-2.5V (Grade 9) used in the Modified Goodman assessment.

Published accelerometer measurements indicate a peak dynamic amplification of approximately 25% above the static mean stress for mountain-bike loading [3]. Taking the mean stress from Equation (5) gives:

$$\sigma_m = 238.6\ \text{MPa}, \qquad \sigma_a = 0.25 \times 238.6 = 59.7\ \text{MPa} \tag{8}$$

Substituting into Equation (7):

$$\frac{59.7}{398} + \frac{238.6}{620} = 0.150 + 0.385 = \mathbf{0.535} \tag{9}$$

The fatigue safety factor is therefore:

$$n_f = \frac{1}{0.535} = \mathbf{1.87} \tag{10}$$

Since $0.535 < 1.0$, the design satisfies the Modified Goodman criterion and is predicted to provide infinite fatigue life ($> 10^7$ cycles) under normal service loading.

4.5 Finite Element Analysis

4.5.1 Model Setup

A static structural FEA study was conducted in SolidWorks 2025 Simulation using the full CAD geometry of the proposed frame. The Ti-3Al-2.5V (Grade 9) alloy was entered as a custom material (Table 9). The rear dropouts were fully constrained and a downward force was applied to the inner bore face of the bottom bracket shell. Two load cases were analysed: 981 N (nominal design load) and 1962 N (double the design load). A curvature-based mesh with 4 mm global element size and 1.5 mm refinement at the bottom bracket shell, head tube and seat-cluster welds was used, consistent with the critical regions identified in published bicycle-frame studies [1, 4].

Property	Symbol	Value	Unit
Elastic modulus	E	93.0	GPa
Poisson's ratio	ν	0.34	–
Yield strength	σ_y	552	MPa
Tensile strength	σ_{UTS}	620	MPa
Mass density	ρ	4480	$\text{kg}\,\text{m}^{-3}$

Table 9: Material properties entered into the SolidWorks 2025 custom material card for Ti-3Al-2.5V (Grade 9).

4.5.2 FEA Results

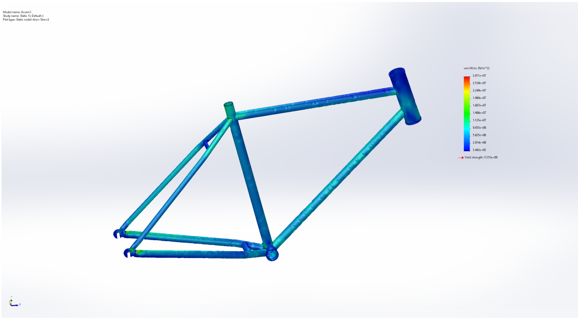

(a) Von Mises stress, 981 N.

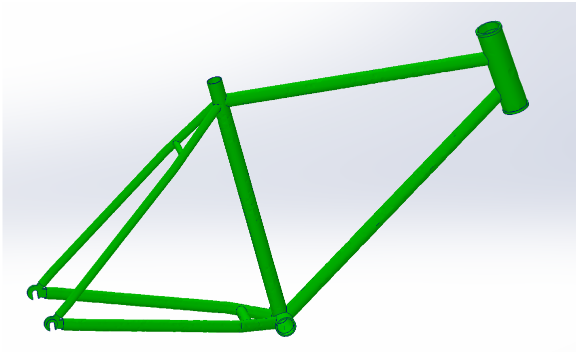

(b) Factor of safety, 981 N.

Figure 7: SolidWorks 2025 FEA results for the nominal 100 kg (981 N) load case: (a) von Mises stress field and (b) factor of safety distribution relative to the 552 MPa yield strength of Ti-3Al-2.5V (Grade 9).

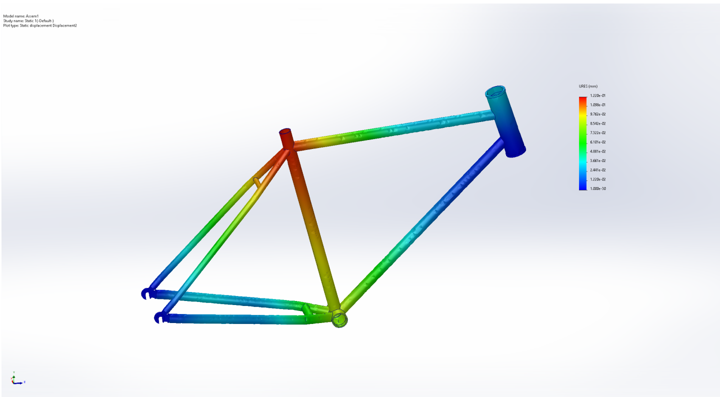

Figure 8: Total displacement (URES) under 981 N applied load. Maximum displacement is **0.122** mm.

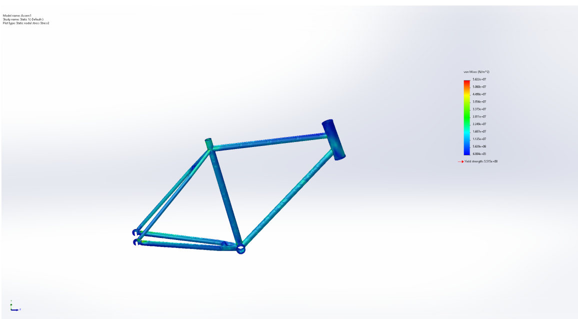

(a) Von Mises stress, 1962 N.

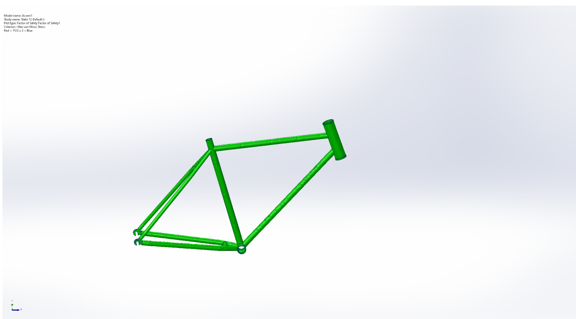

(b) Factor of safety, 1962 N.

Figure 9: SolidWorks 2025 FEA results for the doubled 200 kg (1962 N) qualification load: (a) von Mises stress field and (b) factor of safety distribution.

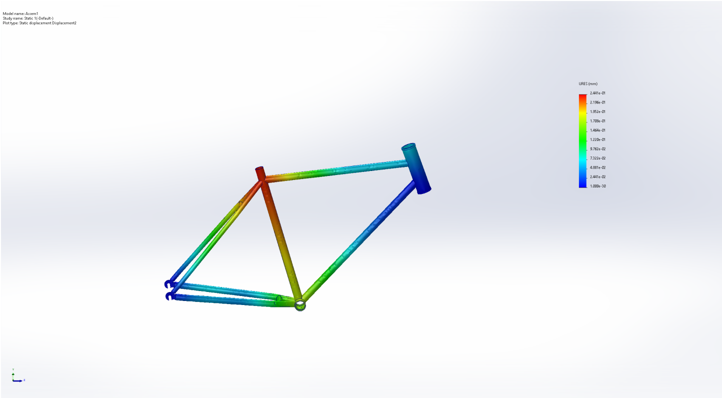

Figure 10: Total displacement (URES) under 1962 N applied load. Maximum displacement is **0.2441** mm.

Across both load cases, the highest stresses occur at the bottom bracket shell-down tube junction and around the head tube, matching critical regions reported in the literature [1, 4]. At 981 N, all regions remain above $n_s = 2.0$ with a maximum displacement of 0.122 mm. At 1962 N, the frame still maintains $n_s \geq 2.0$ throughout, while maximum displacement increases to 0.2441 mm, approximately double the 981 N result and therefore consistent with linear-elastic behaviour. The nominal-load frame safety factor is therefore at least 4.0:

$$n_{s,981\,\mathrm{N}} \geq \mathbf{4.0} \tag{11}$$

4.6 Summary of Quantitative Results

Parameter	**Method**	**Applied load (N)**	$\sigma_{\max}$ **(MPa)**	**Safety factor**
Frame mass	CAD / Eq. (1)	–	–	–
Static bending (down tube)	Beam theory	981	238.6	2.31
ISO 4210 vertical fatigue	Beam theory	1500	356.6	1.55
ISO 4210 combined strength	Beam theory	2200	522.7	1.06
Goodman fatigue ratio	Eq. (9)	–	–	1.87
Full-frame FEA (100 kg)	SolidWorks 2025	981	–	≥ 4.0
Full-frame FEA (200 kg)	SolidWorks 2025	1962	–	≥ 2.0

Table 10: Summary of all quantitative results for the proposed Ti-3Al-2.5V (Grade 9) hardtail mountain-bike frame.

Table 10 summarises the principal numerical outputs. The beam model provides a conservative lower-bound estimate of tube-level stress, whereas the full-frame FEA captures load sharing across the welded diamond frame and therefore predicts a higher global safety factor. Taken together, the results show that the selected Ti-3Al-2.5V frame satisfies the mass, static strength and fatigue requirements of the design brief.

5 Discussion

The main strength of the proposed bicycle-frame design is the clear agreement between material selection, structural analysis and intended service conditions. Ti-3Al-2.5V performs best not because it is the strongest material in isolation, but because it offers the most appropriate balance of low density, corrosion resistance, weldability and fatigue performance for a premium hardtail frame. This is important because bicycle frames are not governed by a single property; they must retain stiffness, resist corrosion in wet off-road use, and survive repeated cyclic loading over a long service life. On that basis, titanium is a more convincing choice than aluminium, magnesium or steel for the present case study.

The most important reason titanium wins is its suitability for a fatigue-dominated application. For a bicycle frame, repeated service loading at welded joints and node regions is more critical than simple static overload. The analytical and numerical results both indicate that the frame is structurally credible under the design load, so the key engineering question becomes durability rather than immediate strength. This aligns with published work showing that frame fatigue depends strongly on node geometry, loading direction and weld quality [1, 5, 18]. Ti-3Al-2.5V is therefore a defensible selection because it combines a favourable endurance limit with excellent resistance to corrosion-assisted crack initiation in wet environments [19].

The FEA also gives useful design insight beyond simple pass/fail assessment. The highest stresses occur at the bottom bracket and head tube, which supports the butting strategy of retaining additional wall thickness at highly loaded junctions while reducing mass in lower-stress spans. This is consistent with the broader mechanics of bicycle frames, where local geometry has a strong effect on stiffness and stress distribution [2]. In that sense, the project shows not just material selection, but also how material can be placed more efficiently through geometry and section design.

The main uncertainty lies in the welded regions. Although the Goodman assessment is useful at concept level, it is based on nominal stresses and does not fully capture weld-toe effects, heat-affected-zone softening, or local manufacturing defects. These are likely to govern real fatigue crack initiation in practice, particularly in a bicycle frame where joints experience complex multiaxial loading [5, 12, 7, 14]. This is also where titanium is least forgiving, because weld shielding, contamination control and purge quality are essential to maintain joint integrity [13, 14].

The next stage of validation should therefore focus on welded-joint durability rather than repeating more static analysis. The most useful improvements would be fatigue-specific FEA using welded-joint S-N data, together with ISO 4210 bench testing and strain-gauge measurement at the bottom bracket and head-tube nodes. Manufacture would also require strict weld shielding, inspection and quality-control procedures consistent with [13, 14, 15]. These steps would provide the evidence needed to move from a strong concept-level design to a more fully verified engineering solution.

6 Conclusion

The goal of this report was to design a metallic bicycle frame for a high-end hardtail rider that is durable, lightweight, and manufacturable. Using Moots as the industry standard, the final suggestion is a butted Ti-3Al-2.5V diamond frame made by precision tube cutting and mitring, local forming, inert-gas welding, alignment control, and finishing. This decision was supported by the alloy's superior ability to connect processing, structure, and performance rather than by cost or tradition.

No single property is suitable on its own, as the material-selection stage demonstrated. AZ31B magnesium is lightweight but less dependable in wet off-road use, 6061-T6 aluminium is suitable for hydroformed mass production but loses appeal if weld-zone fatigue and environmental endurance are prioritised, and steel delivers rigidity and toughness but has a density penalty. With the highest weighted score of 4.20 and exceeding the alternatives in the most important design criteria; fatigue resistance, corrosion resistance, and lifetime durability-Ti-3Al-2.5V was found to be the most balanced option.

This choice is supported by the quantitative analysis. The suggested frame mass is 1.19 kg, which is significantly less than the 5 kg limit. While Goodman's analysis anticipated a fatigue safety factor of 1.87 and unlimited life beyond $> 10^7$ cycles under typical service stress, conservative beam theory yielded a static safety factor of 2.31 at 981 N. Additionally, full-frame FEA revealed safety factors of at least 2.0 at 1962 N and at least 4.0 at 981 N, demonstrating that the welded frame distributes load more efficiently than the simplified beam model predicts.

With all factors considered, Ti-3Al-2.5V offers the best engineering justification for a high-end hardtail frame. To turn the current concept into a fully proven production design, further work should concentrate on welded-joint fatigue modelling, ISO 4210 bench testing, and tighter weld-shielding control.

References

[1] D. Covill, P. Allard, J.-M. Drouet, and N. Emerson, "An Assessment of Bicycle Frame Behaviour under Various Load Conditions Using Numerical Simulations," *Procedia Engineering*, vol. 147, pp. 665–670, 2016, doi: 10.1016/j.proeng.2016.06.269.

[2] D. Covill, A. Blayden, D. Coren, and S. Begg, "Parametric Finite Element Analysis of Steel Bicycle Frames: The Influence of Tube Selection on Frame Stiffness," *Procedia Engineering*, vol. 112, pp. 34–39, 2015, doi: 10.1016/j.proeng.2015.07.172.

[3] M. Melańczuk and P. Maślak, "Determination of Loads Acting on the MTB Bike with the Use of Accelerometers and Strength Calculations of the Frame," *Materials Today: Proceedings*, 2023, doi: 10.1016/j.matpr.2023.09.067.

[4] S. Cicero, R. Lacalle, R. Cicero, D. Fernández, and D. Méndez, "Analysis of the Cracking Causes in an Aluminium Alloy Bike Frame," *Engineering Failure Analysis*, vol. 18, no. 1, pp. 36–46, 2011, doi: 10.1016/j.engfailanal.2010.08.001.

[5] T. Tomaszewski, "Fatigue Life Analysis of Steel Bicycle Frame According to ISO 4210," *Engineering Failure Analysis*, vol. 122, art. no. 105195, 2021, doi: 10.1016/j.engfailanal.2020.105195.

[6] R. C. Soares, E. da Rosa, and A. I. F. Sousa, "Assessment of Fatigue Damage in Welded Aluminum Joints Subjected to Multiaxial Stress State," *Heliyon*, vol. 9, no. 4, art. no. e15196, 2023, doi: 10.1016/j.heliyon.2023.e15196.

[7] R. R. Ambriz, D. Chicot, N. Benseddiq, G. Mesmacque, and S. D. de la Torre, "Local mechanical properties of the 6061-T6 aluminium weld using micro-traction and instrumented indentation," European Journal of Mechanics - A/Solids, vol. 30, no. 3, pp. 307–315, 2011, doi: 10.1016/j.euromechsol.2010.12.007.

[8] J. Liao, M. Hotta, and N. Yamamoto, "Corrosion Behavior of Fine-Grained AZ31B Magnesium Alloy," *Corrosion Science*, vol. 61, pp. 208–214, 2012, doi: 10.1016/j.corsci.2012.04.039.

[9] V. Beura, D. Zhang, N. Overman, J. Darsell, D. R. Herling, K. Solanki, and V. V. Joshi, "Enhanced Mechanical Behavior and Corrosion Resistance of AZ31 Magnesium Alloy Through a Novel Solid-Phase Processing," *Corrosion Science*, vol. 197, art. no. 110074, 2022, doi: 10.1016/j.corsci.2021.110074.

[10] J. C. Williams and R. R. Boyer, “Opportunities and Issues in the Application of Titanium Alloys for Aerospace Components,” *Metals*, vol. 10, no. 6, art. no. 705, 2020, doi: 10.3390/met10060705.

[11] Uniquely Moots - Titanium Bikes Made in Colorado - Moots Cycles. (n.d.). Retrieved March 14, 2026, from https://moots.com/pages/about-us

[12] Ucok, I., Kramer, L. S., Gungor, M. N., Wolfe, P., Dong, H., & Tack, W. T. (2005). Effect of welding on microstructure and tensile properties of flowformed Ti-6Al-4V tubes. Materials Science and Engineering: A, 410–411, 160–164. doi: 10.1016/j.msea.2005.08.174.

[13] F. Javidrad, H. Farghadani, and M. Hedari, “The MPAW of Ti-3Al-2.5V Thin Sheets and Its Effects on Mechanical and Microstructural Properties,” *Journal of Materials Engineering and Performance*, vol. 23, pp. 666–672, 2014, doi: 10.1007/s11665-013-0785-7.

[14] S. Tolvanen, R. Pederson, and U. Klement, “Microstructure and Mechanical Properties of Ti-6Al-4V Welds Produced with Different Processes,” *Materials*, vol. 17, no. 4, art. no. 782, 2024, doi: 10.3390/ma17040782.

[15] Oboh, A. E., Bassey, M. O., & Ikpe, A. E. (2024). Comprehensive study on the effects of TIG welding parameters on the microstructure and mechanical properties of titanium alloys: A review. Mechanical Technology and Engineering Insights, 1(1), 53–70. doi: 10.48313/mtei.v1i1.24.

[16] A. Alaswad, K. Y. Benyounis, and A. G. Olabi, “Tube Hydroforming Process: A Reference Guide,” *Materials and Design*, vol. 33, pp. 328–339, 2012, doi: 10.1016/j.matdes.2011.07.052.

[17] C. Bell, J. R. Corney, N. Zuelli, and D. Savings, “A State of the Art Review of Hydroforming Technology: Its Applications, Research Areas, History, and Future in Manufacturing,” *International Journal of Material Forming*, vol. 13, pp. 789–828, 2020, doi: 10.1007/s12289-019-01507-1.

[18] A. Callens and A. Bignonnet, “Fatigue Design of Welded Bicycle Frames Using a Multiaxial Criterion,” *Procedia Engineering*, vol. 34, pp. 640–645, 2012, doi: 10.1016/j.proeng.2012.04.109.

[19] O. Karpenko, S. Oterkus, and E. Oterkus, “Titanium Alloy Corrosion Fatigue Crack Growth Rates Prediction: Peridynamics Based Numerical Approach,”

International Journal of Fatigue, vol. 162, art. no. 107023, 2022, doi: 10.1016/j.ijfatigue.2022.107023.

[20] Bache, M. R. (2003). A review of dwell sensitive fatigue in titanium alloys: The role of microstructure, texture and operating conditions. International Journal of Fatigue, 25(9–11), 1079–1087. doi: 10.1016/S0142-1123(03)00145-2.

[21] Nascimento, M. P., Voorwald, H. J. C., & Payão Filho, J. D. C. (2011). Fatigue strength of tungsten inert gas-repaired weld joints in airplane critical structures. Journal of Materials Processing Technology, 211(6), 1126–1135. doi: 10.1016/j.jmatprotec.2011.01.016

[22] Koç, M., & Altan, T. (2001). An overall review of the tube hydroforming (THF) technology. Journal of Materials Processing Technology, 108(3), 384–393. doi: 10.1016/S0924-0136(00)00830-X